

## Surprising Hydrodynamic Results Discovered by Means of Direct Simulation Monte Carlo

**Alejandro L. Garcia**

Dept. Physics & Astronomy, San Jose State University and  
Center for Computational Sciences and Engineering, Lawrence Berkeley Nat. Lab.  
USA

[algarcia@algarcia.org](mailto:algarcia@algarcia.org)

### **ABSTRACT**

*These lecture notes describe a variety of interesting physical phenomena discovered by means of Direct Simulation Monte Carlo (DSMC).*

### **1.0 DIRECT SIMULATION MONTE CARLO**

Molecular dynamics (MD) is inefficient for simulating dilute gases at the kinetic scale. The main reason is that the relevant time scale in this regime is the mean free time but the computational time step in MD is limited (by numerical stability) to the collision time. Typically there are many orders of magnitude difference between these time scales and much of the computational effort is wasted during the ballistic motion between collisions. Molecular dynamics, on the other hand, is efficient for liquids since molecules are in a constant state of interaction with their surrounding neighbour molecules.

Direct Simulation Monte Carlo (DSMC) overcomes the inefficiency of MD by replacing the deterministic motion with a stochastic approximation for the collision process. DSMC is able to advance in time steps comparable to the mean free time between collisions yet remain accurate at the level of the Boltzmann equation. Unlike MD, DSMC is always numerically stable regardless of time step.

DSMC was developed by Graeme Bird in the late 1960's and was quickly adopted by the aerospace engineering community because the method is accurate for flows with high Knudsen number (Kn), the ratio of mean free path to system length. In time the method was applied to an expanded number of problems in physics, chemistry, and engineering. Examples range from micron-scale flows (which are also high Knudsen number) to granular gases to lunar atmospheres. The algorithm evolved as well, with improvements to the numerical accuracy and efficiency as well as extensions to complex chemistry and even to dense gases. Nearly 50 years after its introduction DSMC remains the dominant numerical method for molecular simulations of dilute gases.

The details of the DSMC algorithm are presented in detail by Bird [1] and in tutorials [2] (as well as in some of the other lectures in this series) but for the sake of completeness the basic scheme is outlined in this section. DSMC is a particle-based scheme so a typical calculation initializes the desired geometry with boundary conditions and fills the computational volume with random particles. At each time step all particles move ballistically according to their assigned velocity; in DSMC collisions are *independent* of these trajectories. Any particles reaching a boundary are processed according to the imposed conditions, such as randomly assigning a new velocity to a particle that strikes a thermal wall. If there are open boundaries (e.g., wind-tunnel configuration) then particles are generated as inflow and removed if they exit through the boundary.

The core of DSMC is the stochastic (Monte Carlo) evaluation of the collisions. The physical domain is partitioned into "collision cells" and during a time step particles are randomly selected as collision

Report Documentation Page				Form Approved OMB No. 0704-0188	
Public reporting burden for the collection of information is estimated to average 1 hour per response, including the time for reviewing instructions, searching existing data sources, gathering and maintaining the data needed, and completing and reviewing the collection of information. Send comments regarding this burden estimate or any other aspect of this collection of information, including suggestions for reducing this burden, to Washington Headquarters Services, Directorate for Information Operations and Reports, 1215 Jefferson Davis Highway, Suite 1204, Arlington VA 22202-4302. Respondents should be aware that notwithstanding any other provision of law, no person shall be subject to a penalty for failing to comply with a collection of information if it does not display a currently valid OMB control number.					
1. REPORT DATE <b>JAN 2011</b>		2. REPORT TYPE <b>N/A</b>		3. DATES COVERED <b>-</b>	
4. TITLE AND SUBTITLE <b>Review of Rarefied Gas Effects in Hypersonic Applications</b>				5a. CONTRACT NUMBER	
				5b. GRANT NUMBER	
				5c. PROGRAM ELEMENT NUMBER	
6. AUTHOR(S)				5d. PROJECT NUMBER	
				5e. TASK NUMBER	
				5f. WORK UNIT NUMBER	
7. PERFORMING ORGANIZATION NAME(S) AND ADDRESS(ES) <b>Dept. Physics &amp; Astronomy, San Jose State University and Center for Computational Sciences and Engineering, Lawrence Berkeley Nat. Lab. USA</b>				8. PERFORMING ORGANIZATION REPORT NUMBER	
9. SPONSORING/MONITORING AGENCY NAME(S) AND ADDRESS(ES)				10. SPONSOR/MONITOR'S ACRONYM(S)	
				11. SPONSOR/MONITOR'S REPORT NUMBER(S)	
12. DISTRIBUTION/AVAILABILITY STATEMENT <b>Approved for public release, distribution unlimited</b>					
13. SUPPLEMENTARY NOTES <b>See also ADA579248. Models and Computational Methods for Rarefied Flows (Modeles et methodes de calcul des coulements de gaz rarefies). RTO-EN-AVT-194</b>					
14. ABSTRACT <b>These lecture notes describe a variety of interesting physical phenomena discovered by means of Direct Simulation Monte Carlo (DSMC).</b>					
15. SUBJECT TERMS					
16. SECURITY CLASSIFICATION OF:			17. LIMITATION OF ABSTRACT <b>SAR</b>	18. NUMBER OF PAGES <b>10</b>	19a. NAME OF RESPONSIBLE PERSON
a. REPORT <b>unclassified</b>	b. ABSTRACT <b>unclassified</b>	c. THIS PAGE <b>unclassified</b>			

partners within each cell. The number of collision to occur in a cell is determined from the local number density and temperature (although temperature is used indirectly through average relative velocity). A probability that a pair will collide is assigned based on their relative speed and collision cross-section. If the collision occurs then the post-collision velocities of the colliding particles are selected at random, preserving conservation of momentum and energy. If the particles have internal degrees of freedom, there are further details as to the re-assignment of energy; chemical reactions add further steps to the computation.

The most common application of DSMC is in aerospace engineering where high Knudsen number flows are common due to the rarefied gas conditions. Continuum approaches of Computational Fluid Dynamics (CFD) based on the Navier-Stokes equations (and its variants) are not accurate for these so-called “transition” regime flows because the stress tensor and heat flux are not well approximated by linear functions of gradients. Another common application of DSMC is in microscopic flows since the mean free path for air at standard conditions is roughly 0.05 microns. An example of this type of flow occurs in the lubrication layer between the read/write head and the spinning platter of a computer disk drive. [3] The head is lifted from the platter by high pressure region that develops between them as the air is dragged by the spinning platter. Because the sensitivity of the magnetic response varies exponentially with distance, the head-platter spacing is typically less than 20 nanometers and the Knudsen number of the flow is order one.

The next four sections describe four surprising hydrodynamic results that were discovered using Direct Simulation Monte Carlo. A common theme is that the author has worked on all four of these problems.

## 2.0 ANOMALOUS POISEUILLE FLOW

Poiseuille flow is the fluid motion in a confined channel, such as a pipe, driven by a force acting parallel to the channel. The most common type of forcing is a pressure gradient, with the flow directed from high pressure to low. However we will instead consider Poiseuille flow driven by a body force, such as a constant gravitational acceleration. [4] Furthermore, we consider a simple rectangular geometry with thermal walls left and right and with periodic boundary conditions in the other directions (see Figure 1).

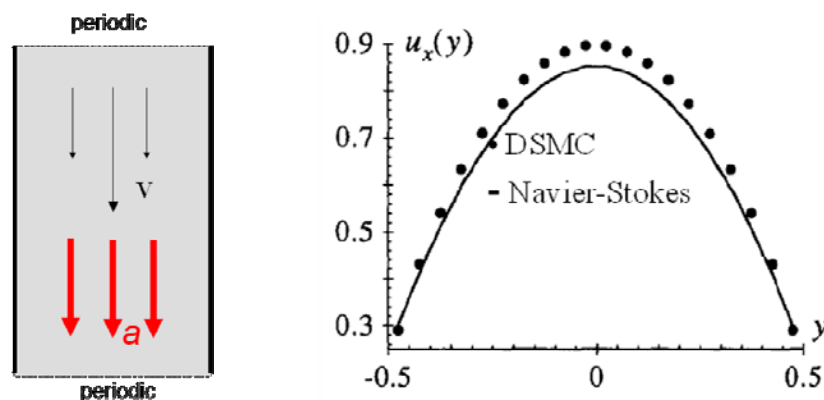


**Figure 1: Acceleration-driven Poiseuille flow; flow geometry (left), fluid velocity (right).**

The acceleration is downward so in this configuration the fluid exits the bottom and is reintroduced at the top; the hydrodynamic variables (fluid velocity, pressure, etc.) only vary in the  $y$ -direction (perpendicular to the walls) at the steady state. This state is reached when the momentum added by the body force is balanced by the momentum removed by the viscous drag of the walls. Similarly, at the steady state the viscous heat produced by the shearing of the fluid is balanced by the cooling of the walls.

From Figure 1 we see that the profile of fluid velocity measured in DSMC is in good qualitative agreement with the quadratic profile predicted by Navier-Stokes (once the slip velocity at the boundary is accounted for) even though the distance between the walls is only 10 mean free paths ( $Kn = 0.1$ ). However the temperature profile (see Figure 2) is qualitatively different in that there is a dip in the centre. Since heat is generated within the gas due to shear and can only be removed at the walls this means that near the centre of the channel heat is flowing *against* the temperature gradient (i.e., flowing from cold to hot).

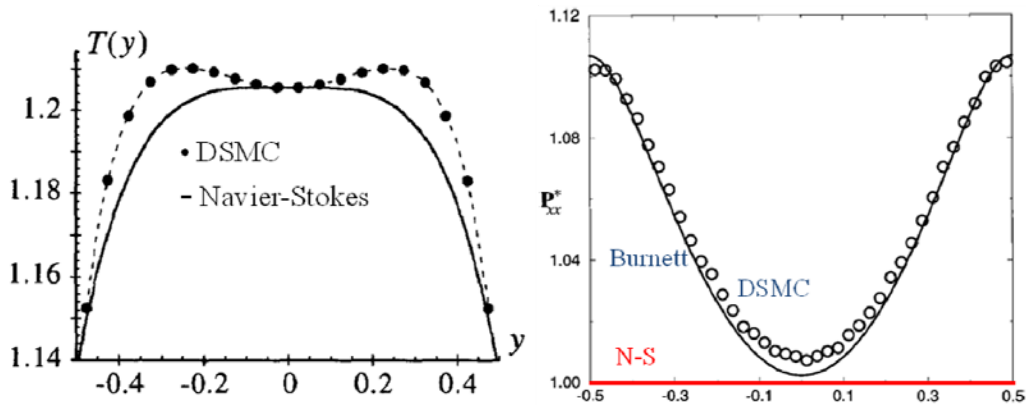


**Figure 2: Acceleration-driven Poiseuille flow; temperature (left), pressure (right).**

The pressure profile is also anomalous in that there is a pressure gradient towards the walls yet at the steady state there cannot be any fluid velocity in this direction. The Navier-Stokes equations have no term in the momentum equation to balance this pressure gradient however at the Burnett level we find agreement with the DSMC measurements. [5] For the temperature profile one has to go to even higher order, namely super-Burnett theory, to obtain the correct profile [6]; the central dip in temperature is also predicted from BGK theory [7]. Finally, pressure-driven driven Poiseuille flow is more complex because the flow is not one-dimensional however similar effects are observed [8]; the profiles of temperature and pressure disagree with Navier-Stokes predictions but are in good agreement with super-Burnett theory [6].

### 3.0 ANOMALOUS COUETTE FLOW

Couette flow is the flow in a confined channel that is driven by a shearing of the fluid created by the motion of the channel walls. In laboratory experiments this is most easily achieved between concentric cylinders with the inner cylinder rotating at a constant angular speed (see Figure 3). There are a number of interesting hydrodynamic instabilities that occur in cylindrical Couette flow however we will restrict our attention to low Reynolds numbers, well below any instability. As in the previous section we consider high Knudsen numbers ( $Kn > 0.1$ ) and investigate the resulting velocity profile of the gas.

The velocity of a gas moving past a solid surface has a velocity at that surface that differs from the surface's velocity, even if the solid fully thermalizes molecules reflecting from it. This effect was predicted by Maxwell and confirmed by Knudsen; the physical origin is the difference between the impinging and reflected velocity distributions of the gas molecules due to gradients. We may define a slip length (see Figure 3), which is the distance within the wall at which the velocity profile of the gas extrapolates to match the wall's velocity. For a fully thermalizing surface the slip length is approximately one mean free path so it is only significant for high  $Kn$  flows. Slip increases if some particles reflect specularly and we define the accommodation coefficient,  $\alpha$ , for a surface as the fraction of thermalized (non-specular) reflections from that surface. [9]

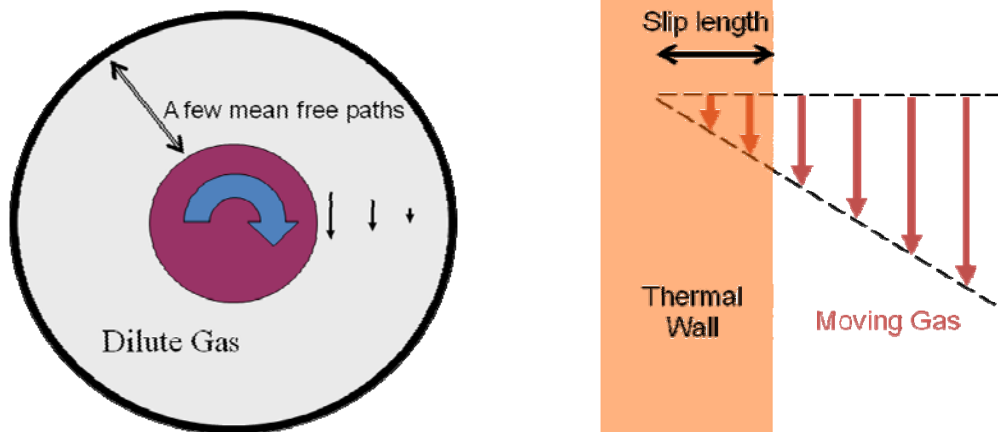


**Figure 3: Cylindrical Couette flow geometry (left); Slip length for a stationary thermal wall (right).**

DSMC simulations of cylindrical Couette flow confirm that when the accommodation coefficient is one (fully thermalizing) the fluid velocity is greatest near the inner (moving) cylinder and decreases with increasing distance from the center (see Figure 4). On the other hand when  $\alpha < 0.1$  the angular speed increases with increasing radial distance; when the walls are nearly completely specular ( $\alpha = 0.01$ ) the gas rotates like a solid body ( $v = \omega r$ ). This result is not anomalous; it was predicted by Maxwell over a century ago as a consequence of the centrifugal force acting as a body force on the fluid.

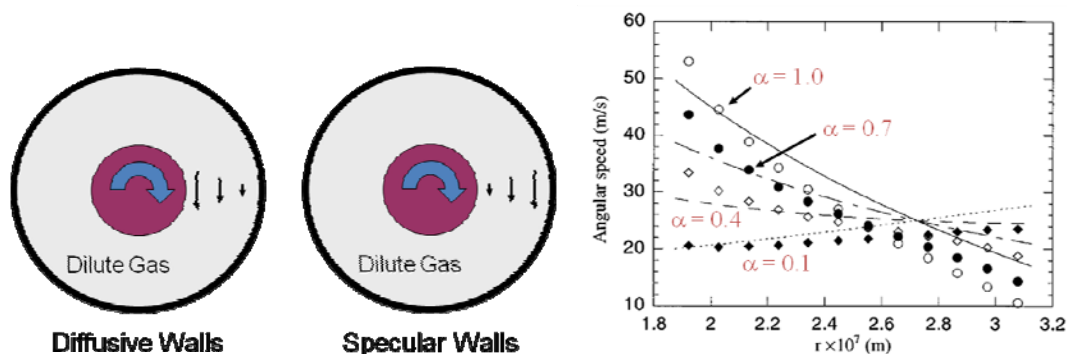


**Figure 4: Couette flow regimes (left); fluid velocity versus radius (right).**

The unexpected result discovered by DSMC is that for a certain range of parameters the fluid velocity has a minimum speed *within* the fluid (see Figure 5). [10] This effect occurs when the walls are 80%-90% specular and has been rigorously confirmed using BGK theory. [11] At present there is no simple physical interpretation for this phenomenon, which involves the interplay of the curved geometry and the asymmetric velocity distribution in the gas. Yet it highlights the unusual and unexpected behaviour that can arise in transition flows.

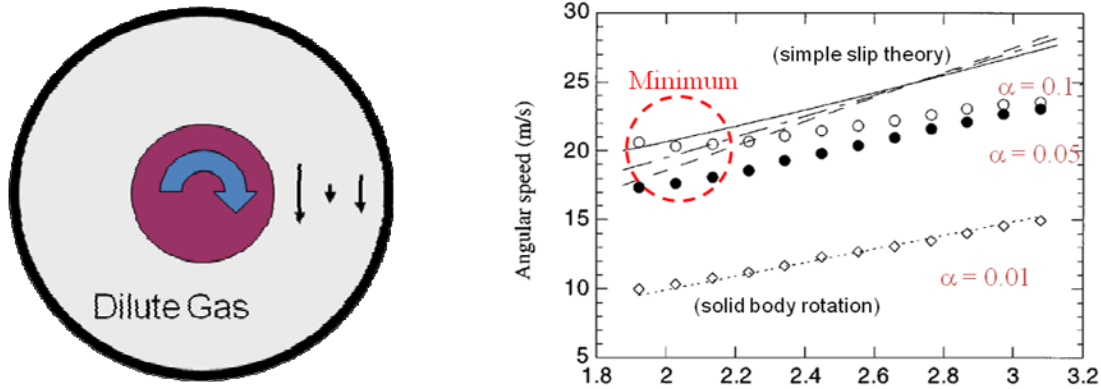


Figure 5: Anomalous Couette flow (left); fluid velocity versus radius (right).

### 3.0 ANOMALOUS TEMPERATURE GRADIENT FLOW

In DSMC, as in all molecular simulations, the computation calculates the positions and velocities of particles as functions of time. But the variables of interest are hydrodynamic quantities, such as pressure and temperature. For some quantities the transformation is unambiguous, for example the mass density is the total mass of particles in a local region divided by the region's volume. Other quantities, such as temperature, entropy, Gibbs free energy, etc., are less obvious. Even fluid velocity has two interpretations.

The intuitive measure of fluid velocity is the average velocity of particles in a local region (i.e., a cell), which we may write as,

$$\bar{v} = \frac{1}{N} \sum_{i \in C} v_i$$

where the sum is over particles within the cell. The same result is obtained from the centre of mass velocity in the cell,

$$u = \frac{J}{M} = \frac{\sum_{i \in C} m v_i}{mN}$$

These two equivalent expressions give the *instantaneous* fluid velocity in the cell; the mean value over  $S$  samples (either time-averages or ensemble-averaged) may be written as,

$$\langle u \rangle = \frac{1}{S} \sum_{j=1}^S u(t_j) = \frac{1}{S} \sum_{j=1}^S \left( \frac{1}{N(t_j)} \sum_{i \in C} v_i(t_j) \right)$$

Yet this is not the only way to define the mean fluid velocity. In fact it is *not* the definition normally used in DSMC. Instead, the mean fluid velocity is calculated as a cumulative average,

$$\langle u \rangle_* = \frac{\sum_j^S \sum_{i \in C}^{N(t_j)} v_i(t_j)}{\sum_j^S N(t_j)}$$

These expressions for the mean fluid velocity are *not* equivalent because the former is the average of a ratio ( $\langle \text{momentum}/\text{mass} \rangle$ ) and the latter is the ratio of the averages ( $\langle \text{momentum} \rangle / \langle \text{mass} \rangle$ ).

Consider a closed box filled with a dilute gas and subjected to a constant temperature gradient imposed by thermal walls. Using the cumulative mean to define fluid velocity, DSMC calculations yield the expected result: no flow at the steady state. However, the mean instantaneous fluid velocity gives an anomalous result: The fluid has a velocity that rises quadratically to a maximum in the centre of the system and the magnitude of this flow varies linearly with the temperature gradient (see Figure 6). [12]

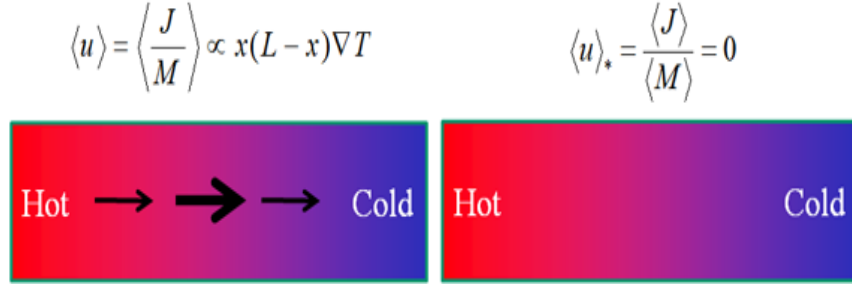


**Figure 6: Anomalous flow in a temperature gradient. Mean instantaneous velocity (left); Cumulative mean fluid velocity (right).**

The physical origin of this effect is that out of equilibrium, as in a temperature gradient, the fluctuations of mass density and of momentum are correlated. At equilibrium, density, fluid velocity, and temperature are conjugate hydrodynamic variables; when measured simultaneously they are uncorrelated. However, out of equilibrium there are asymmetries that produce correlations, which can be computed using Landau-Lifshitz fluctuating hydrodynamics and that are confirmed by DSMC simulations [13]. For example, in a temperature gradient the density fluctuates above average when the fluid velocity fluctuates in the direction against the gradient with; specifically, density and fluid velocity fluctuations are correlated as,

$$\langle \delta \rho(x) \delta u(x) \rangle \propto -x(L-x)\nabla T$$

The two definitions of fluid velocity may be related as,

$$\langle u \rangle \approx \langle u \rangle_* \left( 1 + \frac{\langle \delta N^2 \rangle}{\langle N \rangle^2} \right) - \frac{\langle \delta J \delta N \rangle}{m \langle N \rangle^2} = \langle u \rangle_* - \frac{\langle \delta \rho \delta u \rangle}{\langle \rho \rangle}$$

DSMC simulation results verify that the anomalous fluid velocity is entirely explained by this non-equilibrium correlation of fluctuations.

Finally, it should be noted that a similar bias occurs when using any instantaneous hydrodynamic quantity, such as temperature or pressure.[14] A similar bias is also created if boundary conditions, such as inflow from a reservoir, do not correctly include thermodynamic fluctuations. [15] Because the error goes as  $1/N$ , where  $N$  is the number of particles in the sampling cell, for engineering applications it may be acceptable compared with other approximations. However, it is an effect that all DSMC users should be wary of; we first thought it was a bug in the code!

## 4.0 ANOMALOUS DIFFUSION FLOW

As discussed in the previous section, fluctuations are enhanced when a system is out of equilibrium, such as when a gradient is imposed by boundary conditions. Figure 7 illustrates this effect, showing snap-shots



for an equilibrium system with a concentration gradient induced by gravity and a non-equilibrium system with a comparable concentration gradient imposed by boundary conditions. Clearly the fluctuations are significantly greater in the non-equilibrium steady-state scenario. The effect of fluctuations is even more noticeable in non-steady problems, such as the mixing of initially segregated gases (see Figure 8). These giant fluctuations in diffusive mixing have been observed in laboratory experiments, creating variations visible to the naked eye. [16]

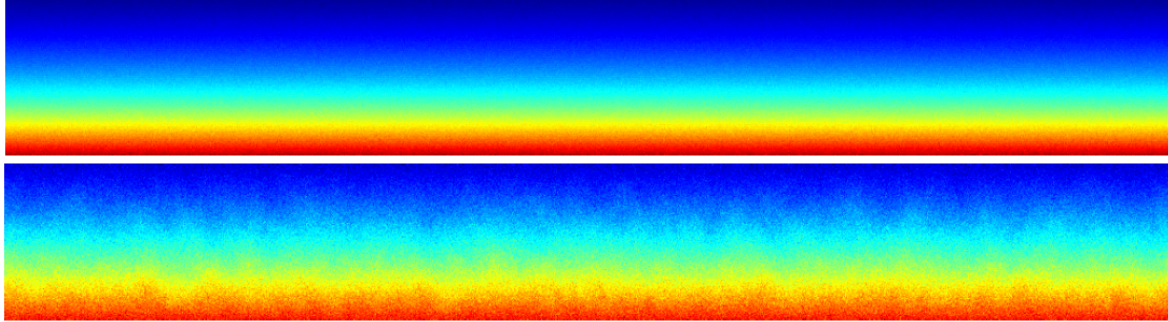


**Figure 7: Equilibrium concentration gradient induced by gravity (above);  
Steady-state concentration gradient imposed by boundary conditions (below)**

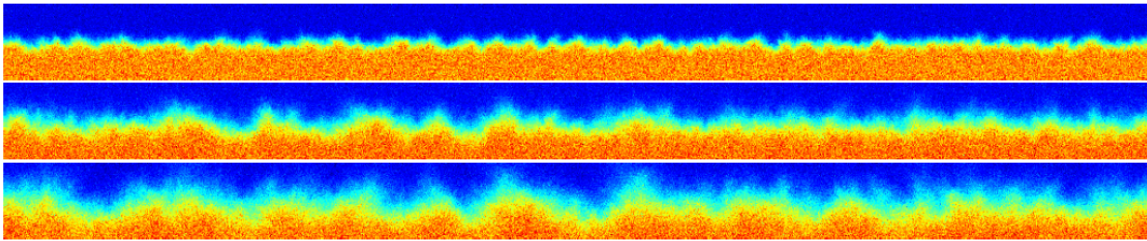


**Figure 8: Snapshots of the concentration in the diffusive mixing of two gases (red and blue) at  
t = 1, 4, 10 (top, middle, bottom), starting from a flat interface (phase-separated system) at t = 0.**

An unexpected consequence of these non-equilibrium fluctuations is that they enhance the effective rate of diffusion. The simplest case is “red-blue” diffusion in which the two species are physically identical. In this case the fluctuations of fluid velocity are the same as in equilibrium. Formulated in terms of fluctuating hydrodynamics the concentration equation is coupled to the velocity; in the isothermal, incompressible approximation the correlation of concentration-velocity fluctuations is, in Fourier space,

$$\langle \tilde{\delta c} \delta \hat{u}_{\parallel} \rangle \propto -\frac{k_{\perp}^2 \nabla c}{k^4}$$

The total mass flux for concentration may be written in the form, [17]

$$\langle j \rangle \approx (D_0 + \Delta D) \nabla c \quad \text{where} \quad \Delta D = -\frac{1}{8\pi^3} \int_k \langle \tilde{\delta c} \delta \hat{u}_{\parallel} \rangle d\mathbf{k}$$

We see that there are two contributions to this flux: the “bare” diffusion coefficient  $D_0$  and the contribution due to the correlation of concentration and velocity fluctuations. Because the latter is also linear in the concentration gradient it may be written as an enhancement to the diffusion coefficient,  $\Delta D$ .



For a slab geometry ( $L_z \ll L_x \ll L_y$ ) we have that  $\Delta D \propto \ln L_x$ . That is, as we make the system wider in a direction perpendicular to the gradient the diffusion is enhanced;  $\Delta D$  increases because the integral over wavenumber extends to smaller values of  $k$  as the system width increases. This enhanced diffusion is anomalous since, in the deterministic hydrodynamics, the diffusion coefficient is independent of the system geometry.

This effect is seen in DSMC simulations where we may separate the contributions to the concentration flux. Specifically, in DSMC we may independently measure the averages and correlations of species density and velocity, as well as total mass flux of each species. As seen in Figure 9, the effective diffusion coefficient increases in qualitative agreement with theory up to system widths approaching the system height ( $L_x \approx L_y$ ). [17]

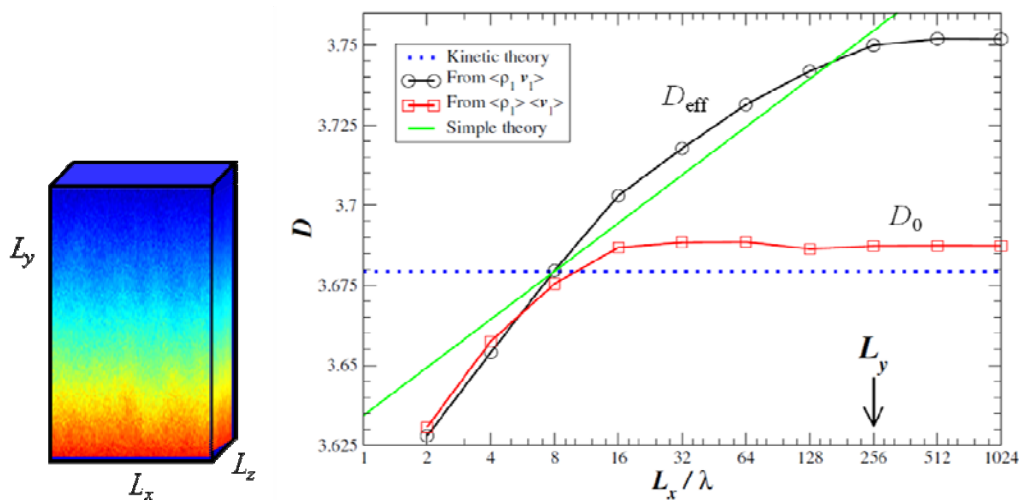


**Figure 9: Simulation geometry (left). DSMC measurements of bare and total effective diffusion coefficients as a function of system width (right)**

## 5.0 CONCLUDING REMARKS

Direct Simulation Monte Carlo is an excellent numerical tool for both applications and for basic research. Given DSMC's computational efficiency even modest resources are adequate; except for the results in Figure 9 all of the results presented in these notes may be reproduced in a day or two using a laptop. Furthermore, DSMC is relatively simple to program and modify; public-domain source codes are available at a number of sites (including the author's). Finally, DSMC is an excellent educational tool for teaching kinetic theory since the algorithm is as simple as molecular dynamics yet is efficient enough to yield basic results, such as the measurement of viscosity for a hard sphere gas, in a matter of minutes.

## 6.0 REFERENCES

- [1] G.A. Bird. *Molecular Gas Dynamics and the Direct Simulation of Gas Flows*. Clarendon (1994).
- [2] F. J. Alexander and A. Garcia, *Computers in Physics*, **11** 588 (1997).
- [3] F. Alexander, A. Garcia and B. Alder, *Physics of Fluids* **6** 3854 (1994).
- [4] M. Malek Mansour, F. Baras and A. Garcia, *Physica A* **240** 255 (1997).

- [5] F. Uribe and A. Garcia, *Physical Review E* **60** 4063 (1999).
- [6] K. Xu, *Physics of Fluids* **15** 2077 (2003).
- [7] M. Tij and A. Santos, *Journal of Statistical Physics* **76** 1399 (1994).
- [8] Y. Zheng, A. Garcia, and B. Alder, *Journal of Statistical Physics* **109** 495-505 (2002).
- [9] C. Cercignani, *Mathematical Methods in Kinetic Theory*, Springer (1990).
- [10] K. Tibbs, F. Baras, A. Garcia, *Physical Review E* **56** 2282 (1997).
- [11] K. Aoki, H. Yoshida, T. Nakanishi, A. Garcia, *Physical Review E* **68** 016302 (2003).
- [12] M. Tysanner and A. Garcia, *Journal of Computational Physics* **196** 173 (2004).
- [13] A. Garcia, *Physical Review A* **34** 1454 (1986).
- [14] A. Garcia, *Communications in Applied Mathematics and Computer Science* **1** 53 (2006).
- [15] M. Tysanner and A. Garcia, *International Journal of Numerical Methods in Fluids* **48** 1337 (2005).
- [16] A. Vailati and M. Giglio, *Nature* **390** 262 (1997).
- [17] A. Donev, A. de la Fuente, J. B. Bell, and A. L. Garcia, *Physical Review Letters* **106** 204501 (2011).

